

Short Communication

Development of an Electrochemical Quartz Crystal Microbalance-Based Immunosensor for C-reactive protein determination

Kai Gao, Song Cui and Sibo Liu *

Department of Critical Care Medicine, Dalian municipal central hospital, Dalian City, Liaolin Province, 116001, P.R. China

*E-mail: siboliu@yeah.net

Received: 14 September 2017 / *Accepted:* 6 November 2017 / *Published:* 16 December 2017

In terms of outcome prediction in patients with inflammation, albumin and C-reactive protein (CRP) at serum levels have been considered to constitute a practical and reliable scoring system. In the present work, highly sensitive detection of C-reactive protein (hs-CRP) was achieved via a new strategy using a quartz crystal microbalance (QCM) immunosensor. A linear relationship was found between the QCM response and CRP concentration (0.04 - 30 $\mu\text{g/mL}$), with a low limit of detection (LOD) maintained via an amplification process.

Keywords: Electrochemical quartz crystal microbalance; Immunosensor; Inflammation Marker; C-reactive protein; Limit of detection

1. INTRODUCTION

Normal plasma lipid levels account for 50% of all myocardial infarctions [1]. The use of risk markers for screening have been reported to provide more favourable identification of high risk patients of cardiovascular events, including Lp(a) lipoprotein, apolipoprotein B-100, apolipoprotein A-I levels, fibrinolytic capacity, and homocysteine and fibrinogen levels. Unfortunately, restricted use has been found for the above risk markers due to prospective data inconsistency, inadequacy of experimental condition standardization, and unconfirmed apparent enhancement of risk prediction resulting from the single involvement of standard lipid screening [2]. Considering the inflammatory process of atherosclerosis [3], some inflammation plasma markers have also been reported to predict coronary event risks, including markers of systemic inflammation occurring in the liver (e.g., serum amyloid A and high-sensitivity C-reactive protein (CRP)), adhesion molecules (e.g., soluble

intercellular adhesion molecule type 1 (sICAM-1)), and cytokines (e.g., interleukin-6) [4-10]. Unfortunately, the above inflammation markers still have an unclear prognostic value, similar to other cardiovascular event risk prediction methods. For instance, inflammation marker levels have been known to vary significantly with time. In addition, the difficulty of measuring all inflammation markers in a single group of patients has been confirmed by previous studies; thus, it is difficult to assess the comparative effectiveness of each marker. Moreover, evidence suggests that results that were used to confirm the significant enhancement in the prediction usefulness of lipid screening by inflammation markers were inadequate and applied only to the case of CRP in middle-aged men [11, 12]. The commercial and standardized measurements for many of the inflammation markers remains to be developed, restricting, to some extent, the use in clinical applications.

In clinical practice, several experiments have been designed for the C-reactive protein, including nephelometric and turbidimetric technologies [13, 14], and enzyme-linked immunosorbent assays (ELISA) [15]. Unfortunately, these techniques suffer from several disadvantages, such as cost ineffectiveness, tendency towards false negatives, low sensitivity, prolonged operation, and undesirable applicability for rapid point-of care determination [16]. Typically, quantification limits of 3–8 mg/L is the primary drawback of routine automated strategies for the quantification of CRP under laboratory conditions [17, 18]. Substantial efforts have been made in the last few decades to develop a strategy with high sensitivity for the prediction of potential coronary event risks of obviously healthy individuals. Surface Plasmon Resonance (SPR) biosensing platforms for CRP have been reported to achieve a LOD of 8 nM (1 µg/mL) of purified CRP, along with a linear range of 16–40 nM (2–5 µg/mL) [19, 20]. Meyer and co-workers [21] proposed a magnetic detection-based strategy, with a linear detection range of 25 to 2500 ng/mL. Kim and co-workers [22] presented an indirect-competitive quartz crystal microbalance immunosensor towards the detection of CRP, with an LOD and linear concentration range of 0.130 ng/mL and 0.130–25,016 ng/mL, respectively. Lee and co-workers [23] reported a chemiluminescence method in a combined microfluidic system for automatic and rapid analysis of CRP protein with an LOD of 0.0125 mg/L. Buch and Rishpon reported a disposable sensor based on protein A and a multiwalled carbon nanotube coated screen-printed electrode for the detection of 0.5 ng/mL CRP. In recent years, several electrochemical impedance spectroscopy (EIS) systems have been involved in CRP analysis. Nevertheless, these impedimetric strategies also have inner drawbacks, which includes: poor sensitivity [24], undesirable specificity [25], or inability of encompassing a clinically relevant range [26, 27].

The present study reported a strategy for the quantitative assay of CRP, where the sensitivity of the quartz crystal microbalance (QCM) immunosensor towards the analysis of CRP was enhanced using gold nanoparticles (AuNP). In addition, the optimization of immunosensor regeneration was carried out during the investigation of sensitivity.

2. EXPERIMENTS

2.1. Reagents and devices

Human C-reactive protein (CRP) and anti-human C-reactive protein antibody (antiCRP) were kindly provided by Sigma–Aldrich. *N*-hydroxysuccinimide (NHS), potassium ferrocyanide

($\text{K}_4\text{Fe}(\text{CN})_6 \cdot 3\text{H}_2\text{O}$), phosphate buffer saline (PBS) tablets, 16-mercapthexanoic acid (16-MUA), 11-mercaptopundecanoic acid (11-MUA), 3,3-dithiodipropionic acid (DTDPA), thiodipropionic acid (TDPA), thiodiglycolic acid (TDGA), thiosalicylic acid (TSA), and thioctic acid (TCA) were commercially available by Sinopharm Group Co. Ltd. 3-Mercaptopropionic acid (MPA), *N*-hydroxysuccinimide (NHS), and *N*-(3-dimethylaminopropyl)-*N'*-ethylcarbodiimide (EDC) were commercially available by Aladdin Co. Ltd. (Shanghai, China). Bovine serum albumin (BSA) was commercially available by Bio science & Technology. Co. Ltd. (Shanghai, China). Human serum albumin (HSA) was commercially available by Wanyumeilan Bio-technology Co. Ltd. (Beijing, China). The present study used a completely automated QCMA-1 biosensor configuration (Sierra Sensors GmbH, Germany) equipped with Au-modified QCMA-1 sensor chips (20 MHz), and two separate spots, which allowed the active and control sensor surfaces to be simultaneously measured. The running buffer flowing rate was set at $25 \mu\text{L min}^{-1}$, and the operating temperature was $25 \text{ }^\circ\text{C}$. Unless otherwise stated, the 3 data points recorded for the measurements were averaged to obtain the data for the present study.

2.2. Sensor chip modification

Initially, plasma etching (50 W power) was carried out on the bare gold sensor chip (QCMA-1). The cleaned chip was submerged into a thiol or sulfide compound solution (5 mM) prepared in absolute ethanol and kept for 1 d. The test thiol solutions included: 3,3-dithiodipropionic acid (DTDPA), thiodipropionic acid (TDPA), thiodiglycolic acid (TDGA), thiosalicylic acid (TSA), thioctic acid (TCA), 11-mercaptopundecanoic acid (11-MUA), and 16-mercaptohexadecanoic acid (16-MUA), all of which were prepared in a 5 mM ethanol solution. This was followed by rinsing the Au chips (ethanol and water subsequently) and drying with nitrogen gas. The as-prepared sensors were stored at $4 \text{ }^\circ\text{C}$ prior to use. To confirm the adsorption of the thiol monolayer on the gold surface, cyclic voltammetry (CV) characterization was carried out with the SAM modified sensor chips in the presence of potassium ferrocyanate (5 mM) 0.1 M KCl. Five cycles of scanning were run for potassium ferrocyanide (0 - 0.5 V) against an Ag/AgCl reference electrode. Stock solutions of 50 mM potassium ferrocyanide were prepared in 0.1 M KCl.

2.3. Immunosensing of CRP

The modified crystal was mounted in the flow cell, with only one side exposed to the solution; the analytical response was also recorded. The detection configuration worked with the aid of a peristaltic pump, and in a continuous flow mode. A total liquid-phase condition for the crystal electrode to reach a baseline was created by injecting PBS (10 mM) into the flow cell at $20 \mu\text{L/min}$. The reflection induced longitudinal waves at the air-liquid interface, which had the potential to affect the crystal resonant frequency. This was prevented by discharging the air bubbles in the liquid phase from the whole tunnel. The non-specific binding sites on the crystal electrode surface were blocked by injecting $100 \mu\text{L}$ of the BSA solution ($100 \mu\text{g/mL}$; in PBS) at $20 \mu\text{L/min}$. This was followed by

another injection of PBS (10 mM) into the flow cell to stabilize the resonance frequency. The injection rate of the CRP sample (50 μL) in PBS was slower, i.e., 5 $\mu\text{L}/\text{min}$. The crystal was slowly washed by PBS at 5 $\mu\text{L}/\text{min}$ after the binding process to obtain another stable frequency. The resonant frequency rapidly decreased after the injection of AuNPs, which conjugated the second anti-CRP antibodies (150 μL) at 5 $\mu\text{L}/\text{min}$, resulting in a further amplification of the antigen-antibody reaction-induced response. PBS was then injected at 5 $\mu\text{L}/\text{min}$ until another stable frequency was obtained. The frequency variation decreased upon equilibrium of the binding process at the given CRP concentrations and eventually becoming stable. The amount of CRP bound on the crystal surface suggested the frequency change.

3. RESULTS AND DISCUSSION

The applied sensor platform was the bare Au QCMA-1 sensor chips. The chip was modified with thiol molecules with varying lengths to generate a self-assembled monolayer (SAM), and CV analysis was performed in the presence of potassium ferrocyanide for the layer generated on the sensor surface. An Au-thiolate bond formed with the Au surface of the sensor chip with the tail carboxyl group exposed to the monolayer-liquid or monolayer-air interface, which contributed to the strong orientation of the thiol monolayer [28]. The bare Au chip before and after absorbing varying thiol compounds was characterized via the CVs, as shown in Fig. 1. A reversible CV was recorded for the bare gold electrode, which suggested that the Au surface was clean. Thereafter, the ferrocyanide ions could interact with the surface of the electrode. These observations are robust and reproducible across numerous assays. We believe them to be general and, from a practical perspective, to have considerable value in the construction of optimally responsive interfaces [29].

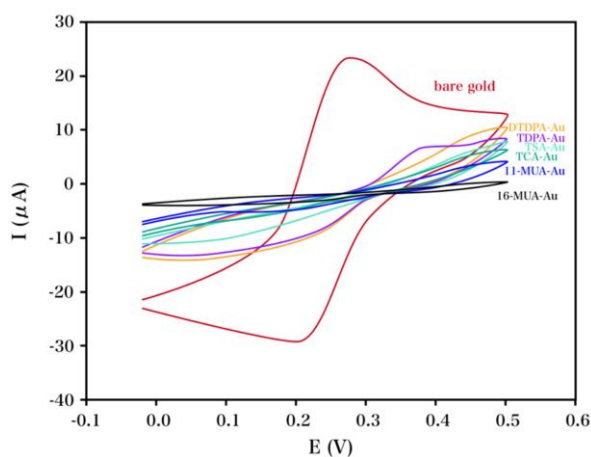


Figure 1. Cyclic voltammetry (CV) characterization recorded for the QCMA-1 sensor chip before and after absorbing 5 mM thiol solutions; bare gold, 3,3-dithiodipropionic acid (DTDPA), thiodipropionic acid (TDPA), thiosalicylic acid (TSA), thioctic acid (TCA), 11-mercaptopundecanoic acid (11-MUA) and 16-mercaptohexadecanoic acid (16-MUA).

A significant insulation surface was created after the MUA-monolayer was formed on the Au electrode, blocking nearly all the faradic currents. Nevertheless, the insulation performance of the modified Au electrode with short-chain thiols, DTDPA, TDPA, TDGA, TSA, and TCA was undesirable, which suggested less surface coverage. Thus, 11-MUA- and 16-MUA-modified chips could be applied for the immobilization of the antibody. Pointedly, we have considered the possibility that the initial resistance plays a role in the subsequent observed sensitivity. Since, the assay is based on the increased charge transfer resistance, one might logically expect sharper increases, and greater assay sensitivity if the receptor layer is initially of comparatively low resistance [29]. The present study chose the 11-MUA-modified chips as the thiol surface and was used in the following measurements. The sensor chip was docked in the QCMA-1 instrument after absorbing thiol (11-MUA) onto the Au surface. The sensor surface was wetted by priming the sensor chip using running buffer under a continuous buffer flow rate of 80 $\mu\text{L}/\text{min}$. Finally, traditional EDC-NHS (N-(3-dimethylaminopropyl)-N'-ethylcarbodiimide/N-hydroxysuccinimide) coupling was used to immobilize the anti-CRP capture monoclonal antibody and mouse IgG onto the active and control sensor array, respectively [30].

The measurement was optimized using varying concentrations, which considered the significance of effective immobilization of the antibody in the sensitive determination of the antigen. Four different concentrations of antibody, over a range of 50 $\mu\text{g}/\text{mL}$ - 200 $\mu\text{g}/\text{mL}$, were prepared in an acetate/acetic acid buffer (pH 5.0) with EDC-NHS (0.1 M), and the 11-MUA modified sensor chips; the injection time was optimized at 3 min. The relationship of frequency shift vs. the antibody concentration increase is shown in Fig. 2. The response shift reached the maximal value (750 Hz) at an antibody concentration of 200 $\mu\text{g}/\text{mL}$; therefore, this concentration was used for CRP binding measurements. The trend in assay sensitivity with the initial layer charge transfer resistance. Notably, as the antibody surface coverage decreased, assay sensitivity initially increased. To cut down the measurement cost, no further study was carried out at increased antibody concentration.

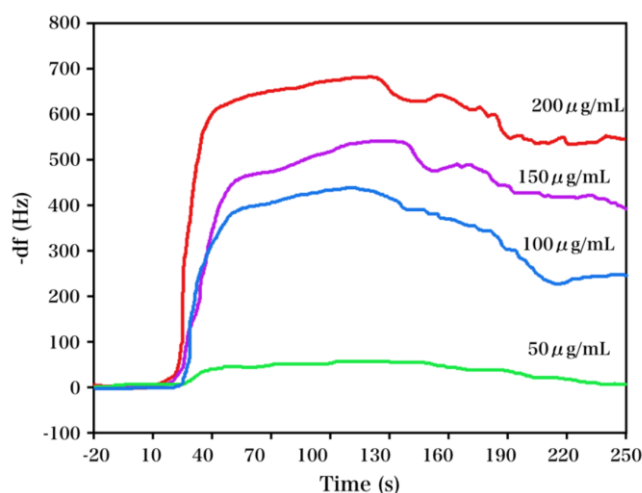


Figure 2. Frequency response patterns recorded for the QCMA-1 immunosensor after absorbing 11-MUA with the EDC/NHS activation reaction on the gold sensor chip and immobilization with varying antibody concentration (50, 100, 150 and 200 $\mu\text{g}/\text{mL}$).

The effect of flow rate on the reaction between antigen and antibody and the sandwich measurement during the injection of CRP antigen, AuNPs, and PBS washing was also studied. The flow rate of the homemade configuration was detected by injecting the samples at varying flow rates (3, 5, 7, 10 and 20 $\mu\text{L}/\text{min}$). Fig. 3 also indicated the assessment of increased frequency shifts. Considering the assay time, 5 $\mu\text{L}/\text{min}$ was selected as the optimized flow rate.

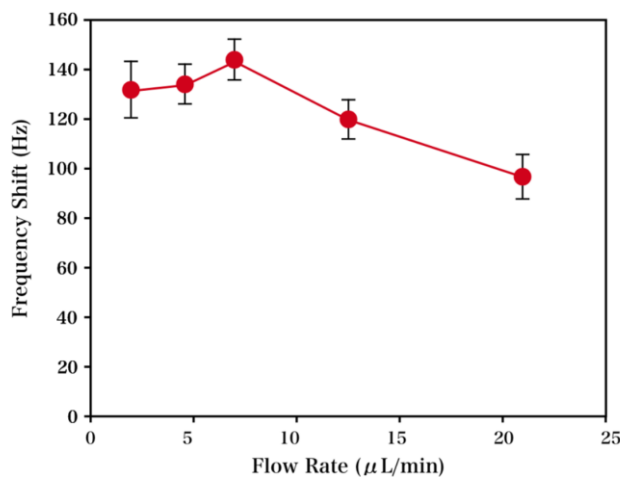


Figure 3. Relationship of increased frequency shifts vs. different flow rates during the determination of CRP (10 $\mu\text{g}/\text{mL}$).

The optimization of the anti-CRP antibody concentration was carried out by incubating the modified electrode in anti-CRP antibody solutions over a concentration range of 0.1 mg/mL - 3 mg/mL . The concentration of anti-CRP antibody, with increased frequency change, is shown in Fig. 4. An increase in the frequency change was observed with the increase in the concentration of anti-CRP antibody, leading to enhancement of the efficiency and sensitivity of our proposed immunosensor. Nevertheless, no apparent response variation was found as the concentration of anti-CRP antibody was further increased over 2 mg/mL , due to the saturation of the SAM layer upon the immobilization of the anti-CRP antibodies. To obtain the optimized immobilization of the anti-CRP antibodies onto the surface of QCM electrode, the optimal concentration was determined to be 2 mg/mL , considering both the material cost and sensitivity. The effects of incubation temperature and incubation time on the QCM response of the immunosensor were also investigated. The results revealed that the response increased with the increase of incubation temperature from 20 to 45 $^{\circ}\text{C}$ and a maximum was obtained at 37 $^{\circ}\text{C}$ [31].

The sensitivity of the QCM immunosensors were investigated using CRP solutions at decreasing concentrations (100 $\mu\text{g}/\text{mL}$ to 20 ng/mL), with the AuNPs responses recorded in Fig. 5A. The modification process was the primary contributing factor in response enhancement (Fig. 5). Different concentrations were applied in evaluating the sensitivity of our proposed sensor. For the repeatability study, each concentration experiment was carried out in triplicate. Fig. 5B displayed a result range of 0.04–100 $\mu\text{g}/\text{mL}$, and the visible nonlinearity with a CRP concentration of 30 $\mu\text{g}/\text{mL}$

was observed in the corresponding plot. Alternatively, calibration curves were plotted with CRP antigen at different concentrations from 0.02 to 30 $\mu\text{g/mL}$.

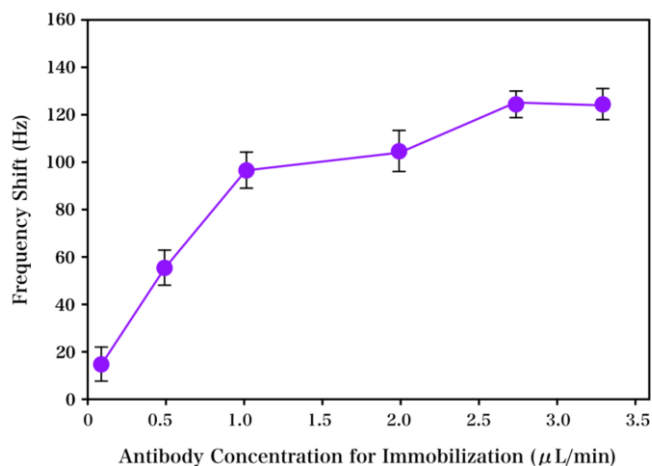


Figure 4. Concentration influence of the anti-CRP antibody on the response of the immunosensor. Frequency shifts in response to the sandwich assays during the incubation of QCM in anti-CRP antibody solutions at varying concentrations for the determination of CRP (10 $\mu\text{g/mL}$).

The frequency responses vs. the above concentration ranges were plotted for the quantification of the modification conjugation induced amplification, along with the antibody-antigen binding induced response. An almost linear proportion was found between the amplified response (ΔF) of our proposed sensor and the concentration of CRP (C) over a range of 0.04–30 $\mu\text{g/mL}$; the LOD and frequency shift were 0.02 $\mu\text{g/mL}$, and 4 Hz \pm 1 Hz, respectively. Therefore, the modification was confirmed to have significantly improved the sensitivity of the immunosensor. To allow for realistic comparison with previous reports, the characteristics of different electrochemical sensors for clenbuterol are summarized in Table 1.

Table 1. Comparison of the major characteristics of the proposed QCM sensors with previous reports for determination of CRP protein.

Electrode	Linear detection range	Detection limit	Reference
ZnO nanotubes	2–60 nM	0.7 nM	[32]
Carbon nanofiber	5–40 nM	2.1 nM	[18]
Chemiluminescence determination	1–100 nM	0.4 nM	[33]
GQD-based CRP biosensor	0.5–70 nM	170 pM	[34]
QCM sensor	0.04–100 $\mu\text{g/mL}$	0.02 $\mu\text{g/mL}$	This work

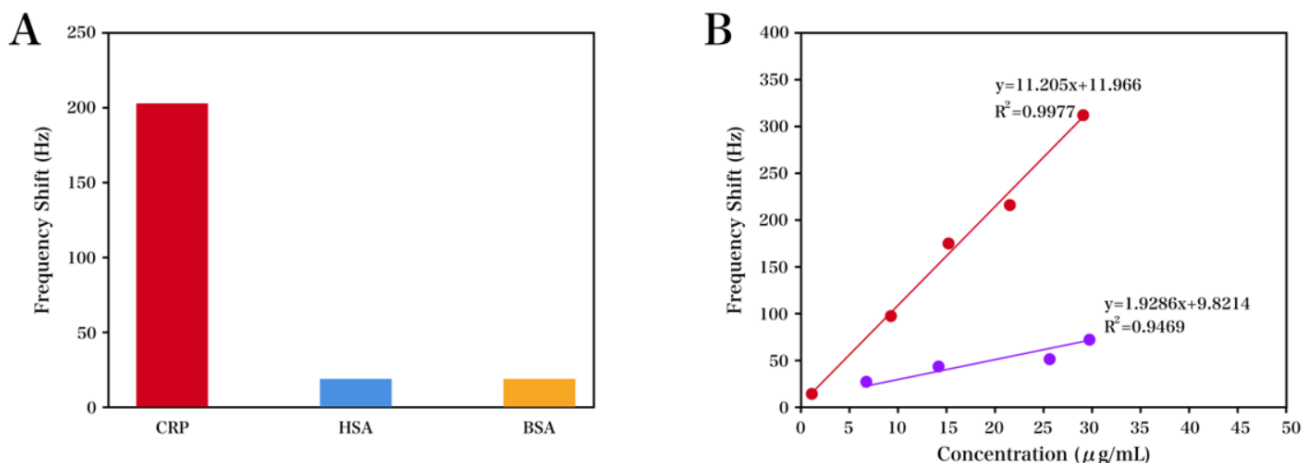


Figure 5. Amplified response comparison of the QCM sensor to CRP (15 µg/mL), HAS (100 µg/mL), and BSA (100 µg/mL). (B) Frequency shift as a function of CRP antigen concentration (a) in the presence and (b) in the absence of conjugation.

As shown in Table 2, the data for the six sera of blood specimens obtained from ELISA and the QCM D technique were compared, together with their relative deviations, to study the accuracy of CRP detection. The relative error was in the range of 2.6% to 3.6%. Thus, it could be concluded that the two methods were desirably coherent with each other. Hence, the requirements of a CRP electrochemical sensor could be well met by the design of the proposed technique to serve for clinical analysis.

Table 2. Experimental results comparison of varied analytical techniques obtained for blood specimens.

Blood samples	1	2	3	4	5	6
Added (µg/mL)	2	2	4	4	8	8
Proposed QCM sensor in this work (µg/mL)	2.02	2.03	3.97	4.01	8.05	8.03
ELISA (µg/mL)	2.02	2.02	4.04	4.03	8.03	8.02
Recovery (%)	101	101.5	99.25	100.25	100.63	100.38
Relative deviation (%)	3.4	2.9	3.1	3.6	2.8	2.6

4. CONCLUSIONS

The present study reported specific, sensitive and rapid determination of CRP using a QCMA-1 immunosensor with nanoparticle amplification and a low LOD (0.02 µg/mL). The results confirmed that the sensitivity of the QCM immunosensor towards the determination of the biomarker could be effectively enhanced using nanoparticle-antibody conjugates. The response of the QCM immunosensor towards the determination of CRP using the nanoparticle amplification strategy was better than that of direct analysis techniques.

References

1. P. Ding, R. Liu, S. Liu, X. Mao, R. Hu and G. Li, *Sensors and Actuators B: Chemical*, 188 (2013) 1277.
2. N. Bijmens, V. Vermeeren, M. Daenen, L. Grieten, K. Haenen, S. Wenmackers, O.A. Williams, M. Ameloot, M. Vandeven and L. Michiels, *physica status solidi (a)*, 206 (2009) 520.
3. W. Chaocharoen, W. Suginta, W. Limbut, A. Ranok, A. Numnuam, P. Khunkaewla, P. Kanatharana, P. Thavarungkul and A. Schulte, *Bioelectrochemistry*, 101 (2015) 106.
4. H.-J. Jang, I.-H. Cho, H.-S. Kim, J.-W. Jeon, S.-Y. Hwang and S.-H. Paek, *Sensors and Actuators B: Chemical*, 155 (2011) 598.
5. B.B. Kim, W.J. Im, J.Y. Byun, H.M. Kim, M.-G. Kim and Y.-B. Shin, *Sensors and Actuators B: Chemical*, 190 (2014) 243.
6. Y. Rasmi, S. Raeisi, S. Mohammadzad and H. Mir, *Helicobacter*, 17 (2012) 116.
7. S. Centi, S. Tombelli, M. Puntoni, C. Domenici, M. Franek and I. Palchetti, *Talanta*, 134 (2015) 48.
8. S. Kurosawa, H. Aizawa, M. Tozuka, M. Nakamura and J.-W. Park, *Measurement Science and Technology*, 14 (2003) 1882.
9. F. Olasagasti and J.C.R. de Gordo, *Translational Research*, 160 (2012) 332.
10. S.K. Mishra, R. Pasricha, A.M. Biradar and Rajesh, *Applied Physics Letters*, 100 (2012) 053701.
11. H.W. Choi, Y. Sakata, T. Ooya and T. Takeuchi, *Journal of bioscience and bioengineering*, 119 (2015) 195.
12. J.-Y. Park, Y.-S. Lee, B.H. Kim and S.-M. Park, *Analytical chemistry*, 80 (2008) 4986.
13. W.L. Roberts, R. Sedrick, L. Moulton, A. Spencer and N. Rifai, *Clinical Chemistry*, 46 (2000) 461.
14. W.L. Roberts, L. Moulton, T.C. Law, G. Farrow, M. Cooper-Anderson, J. Savory and N. Rifai, *Clinical chemistry*, 47 (2001) 418.
15. E.M. Macy, T.E. Hayes and R.P. Tracy, *Clinical chemistry*, 43 (1997) 52.
16. T.A. Pearson, G.A. Mensah, R.W. Alexander, J.L. Anderson, R.O. Cannon, M. Criqui, Y.Y. Fadl, S.P. Fortmann, Y. Hong and G.L. Myers, *Circulation*, 107 (2003) 499.
17. X. Bing and G. Wang, *Int. J. Electrochem. Sci*, 12 (2017) 6304.
18. R.K. Gupta, A. Periyakaruppan, M. Meyyappan and J.E. Koehne, *Biosensors and Bioelectronics*, 59 (2014) 112.
19. C. Kokkinos, M. Prodromidis, A. Economou, P. Petrou and S. Kakabakos, *Analytica chimica acta*, 886 (2015) 29.
20. J. Wang, J. Guo, J. Zhang, W. Zhang and Y. Zhang, *Biosensors and Bioelectronics*, 95 (2017) 100.
21. M.H.F. Meyer, M. Hartmann, H.-J. Krause, G. Blankenstein, B. Mueller-Chorus, J. Oster, P. Miethel and M. Keusgen, *Biosensors and bioelectronics*, 22 (2007) 973.
22. N. Kim, D.-K. Kim and Y.-J. Cho, *Sensors and Actuators B: Chemical*, 143 (2009) 444.
23. W.-B. Lee, Y.-H. Chen, H.-I. Lin, S.-C. Shiesh and G.-B. Lee, *Sensors and Actuators B: Chemical*, 157 (2011) 710.
24. M. Buch and J. Rishpon, *Electroanalysis*, 20 (2008) 2592.
25. P. Tripathi, C.R.P. Patel, A. Dixit, A.P. Singh, P. Kumar, M.A. Shaz, R. Srivastava, G. Gupta, S.K. Dhawan and B.K. Gupta, *Rsc Advances*, 5 (2015) 19074.
26. Y. Zhang, C.R.P. Fulong, C.E. Hauke, M.R. Crawley, A.E. Friedman and T.R. Cook, *Chemistry-A European Journal*, 23 (2017) 4532.
27. R.K. Gupta, R. Pandya, T. Sieffert, M. Meyyappan and J.E. Koehne, *Journal of Electroanalytical Chemistry*, 773 (2016) 53.
28. C.D. Bain, E.B. Troughton, Y.T. Tao, J. Evall, G.M. Whitesides and R.G. Nuzzo, *Journal of the American Chemical Society*, 111 (1989) 321.
29. T. Bryan, X. Luo, P.R. Bueno and J.J. Davis, *Biosensors and Bioelectronics*, 39 (2013) 94.
30. I.-S. Park, D.-K. Kim, N. Adanyi, M. Varadi and N. Kim, *Biosensors and Bioelectronics*, 19 (2004) 667.

31. X. Wang, J. Zhang and Z. Zheng, *Sensor Letters*, 11 (2013) 1617.
32. Z.H. Ibupoto, N. Jamal, K. Khun and M. Willander, *Sensors and Actuators B: Chemical*, 166 (2012) 809.
33. S. Wang, E. Harris, J. Shi, A. Chen, S. Parajuli, X. Jing and W. Miao, *Phys Chem Chem Phys*, 12 (2010) 10073.
34. X. Bing and G. Wang, *Int. J. Electrochem. Sc.*, 12 (2017) 6304

© 2018 The Authors. Published by ESG (www.electrochemsci.org). This article is an open access article distributed under the terms and conditions of the Creative Commons Attribution license (<http://creativecommons.org/licenses/by/4.0/>).